Chapter 11
Study of STATCOM in *abc* Framework

Juan M. Ramirez, Juan Miguel Gonzalez-Lopez, Julio C. Rosas-Caro, Ruben Tapia-Olvera, Jose M. Lozano and Antonio Valderrabano-Gonzalez

Abstract In this chapter, the STATCOM characteristics are analyzed when it is utilized for improving the voltage stability. This chapter aims to analyze the STATCOM in the *abc* coordinates, and its impact over the power system under steady state and transient conditions is studied. Mathematical description of the main components is included to represent the dynamic behavior. These elements are formulated by differential equations in order to demonstrate how the STATCOM influences overall power system performance and voltage stability margins. The proposed methodology is validated on a Synchronous Machine Infinite Bus (SMIB) and on the New England test power system, which comprises 39-buses, 46-transmission lines, and 10-generators.

J.M. Ramirez (✉)
Centro de Investigacion y de Estudios Avanzados del Instituto Politecnico Nacional,
Av. del Bosque 1145, Col. el Bajio, 45019 Zapopan, JAL, Mexico
e-mail: jramirez@gdl.cinvestav.mx

J.M. Gonzalez-Lopez
Universidad Tecnologica de Manzanillo, Camino hacia las humedades s/n, Col. Salagua,
28869 Manzanillo, COL, Mexico
e-mail: jmgonzalez@utmanzanillo.edu.mx

J.C. Rosas-Caro · A. Valderrabano-Gonzalez
Universidad Panamericana, Campus Guadalajara, Czda Circ Poniente No. 49,
Col. Cd Granja, 45010 Zapopan, JAL, Mexico
e-mail: crosas@up.edu.mx

A. Valderrabano-Gonzalez
e-mail: avalder@up.edu.mx

R. Tapia-Olvera
Universidad Politecnica de Tulancingo, Calle Ingenierias No. 100. Col. Huapalcalco,
43629 Tulancingo, HGO, Mexico
e-mail: ruben.tapia@upt.edu.mx

J.M. Lozano
Division de Ingenierias, Universidad de Guanajuato, Campus Irapuato-Salamanca,
Carr. Salamanca—V. de Santiago, Comunidad de Palo Blanco, 36885 Salamanca
GTO, Mexico
e-mail: jm.lozano@ugto.mx

F. Shahnia et al. (eds.), *Static Compensators (STATCOMs) in Power Systems*,
Power Systems, DOI 10.1007/978-981-287-281-4_11

Keywords Power system voltage stability · PV-curves · STATCOM · Voltage stability margin

11.1 Introduction

Figure 11.1a shows a basic representation of a radial power system to define its different electric parameters; a bus feeds a load through a transmission line.

The active and reactive power transfer between power source and load depends on the voltage magnitude in both bus and phase angles; Fig. 11.1a shows the power triangle corresponding to the load bus. P, Q and S represent active, reactive and apparent power, respectively. From the power triangle, the power factor may be expressed by

$$P.F. = \frac{P}{S} = \frac{P}{\sqrt{P^2 + Q^2}} = \cos\phi \tag{11.1}$$

Figure 11.1a is used to relate the active power, reactive power and the voltage in the load bus; the generator or system voltage is assumed constant and it is taken as the reference bus. The line impedance is represented by its series inductive reactance jX, assuming a lossless system, neglecting the line capacitance; all variables are expressed in per unit, pu This small system uses the Thévenin equivalent to the power system seen from the load bus.

The bus voltage is given by the expression:

$$\tilde{V} = \tilde{E} - jX\tilde{I} \tag{11.2}$$

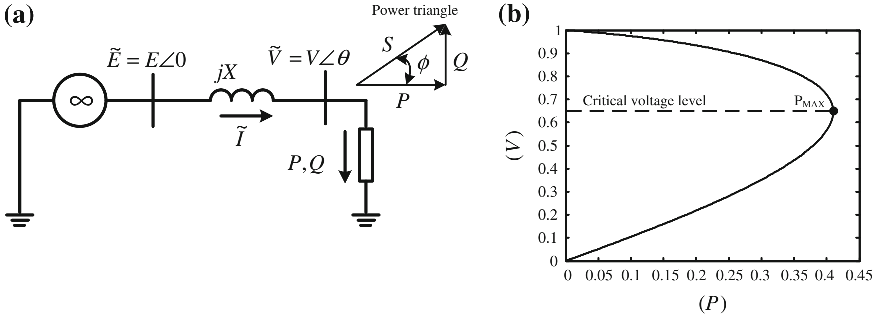

Fig. 11.1 **a** Basic radial power system. **b** PV curve considering $\tan\phi = 0.6$

The active and reactive power delivered to the grid can flow in both directions either absorbed or generated. This equation contains both of them, and may be expressed by:

$$S = P + jQ = \tilde{V}\tilde{I}^{*} = \tilde{V}\,\frac{\tilde{E}^{*} - \tilde{V}^{*}}{-jX} = \frac{j}{X}\left(EV\cos\theta + jEV\mathrm{sen}\theta - V^{2}\right) \tag{11.3}$$

The complex power may be separated into the active and reactive component as

$$P = -\frac{EV}{X}\mathrm{sen}\theta; \qquad Q = -\frac{V^{2}}{X} + \frac{EV}{X}\cos\theta \tag{11.4}$$

Equation (11.4) relate the P and Q values to the magnitude V and phase θ of voltage, the angle is normally small providing a close relationship between the load-bus voltage and the reactive power, and a close relationship between the phase angle and the active power [1, 2]. This decoupled behavior holds during normal operation, and not during extreme load operations [3].

It is possible to handle the phase angle θ by an algebraic procedure and write

$$\left(V^{2}\right)^{2} + \left(2QX - E^{2}\right)V^{2} + X^{2}\left(P^{2} + Q^{2}\right) = 0 \tag{11.5}$$

From this second order equation, the necessary condition to have a solution becomes

$$-P^{2} - \frac{E^{2}}{X}Q + \left(\frac{E^{2}}{2X}\right)^{2} \geq 0 \tag{11.6}$$

Assuming this constraint, there are two possible solutions for (11.5),

$$V = \sqrt{\frac{E^{2}}{2} - QX \pm \sqrt{\frac{E^{4}}{4} - X^{2}P^{2} - XE^{2}Q}} \tag{11.7}$$

According to the power triangle, Fig. 11.1a, the reactive power can be also expressed by

$$Q = P\,\tan\phi \tag{11.8}$$

Once the phase angle has been eliminated from the formulation, the only unknown parameter is the voltage magnitude V; it can be solved since E and X are constants. According to (11.8), Q depends on P, and considering a constant power factor, V depends only on P.

11.1.1 PV-Curves

The relationship between the active power P and the voltage magnitude V is quite important in voltage stability analysis, and their interaction is depicted in the *PV*-curves. For the analyzed case, such curves can be obtained once both solutions (11.5) are known.

A PV-curve for the radial system is depicted in Fig. 11.1b, when tan $\phi = 0.6$. As above mentioned, for a given power factor, (11.5) has two possible solutions:

1. The one achieved considering a positive sign, results in an operative condition where V is relatively high and the current I is relatively small, which is the segment of the curve shown in Fig. 11.1b above the dotted line; this is the desired operating range.
2. The second solution corresponds to the negative sign, producing an operation bellow the dotted line in Fig. 11.1b, with a low voltage V and a high current I; this is an undesired operation where the systems becomes unstable.

In Fig. 11.1b, the point of $V = 1$ pu (left upper corner) corresponds to the lower load condition. Increasing the load, the voltage decreases gradually approaching to the maximum power transfer point $P_{\max}$. This operating point has different definitions in the voltage stability analysis, for instance, *critical voltage point* or *voltage collapse point*. When the system is operating near this point, a small load increment may produce a high voltage reduction, and after the critical voltage, any increment on the current leads to an unstable operation.

To explain the way power $P_{\max}$ can be calculated, let's assume the load power behaves as impedance. The problem can be formulated by the maximum power transfer theorem, which indicates the maximum power transfer is reached when the load impedance is equal in magnitude to the Thévenin systems impedance [4].

PV-curves are useful to conceptually analyze the voltage stability problem in radial systems. Figure 11.2a shows other PV-curves for the same system shown in Fig. 11.1a but for different power factors. The curves are normalized to the short-circuit power of the system (E^2/X); each curve corresponds to a different power factor.

The power factor has an important effect in the voltage-power characteristic. Another important aspect is when the power factor is leading (tan $\Phi < 0$), that means the load is capacitive or there is a parallel compensation. In this case, the maximum power point $P_{\max}$ increases with respect to the lagging power factor and the voltage magnitude. This is because for negative values of tan(Φ), an increment in the load active power produces an increment in the reactive power produced by the load (or parallel compensator). This situation is difficult to identify because the maximum power-transfer point can be reached when the voltage has a normal magnitude, hiding the real system's condition.

So far, only the load active power versus voltage magnitude has being described, with a constant power factor. In this case, according to (11.8), each value of P corresponds to a value of Q. The reactive power load is analyzed through Fig. 11.2b,

Fig. 11.2 **a** PV-curves for different power factors. **b** Voltage versus active and reactive power. **c** Voltage stability margin of a power system

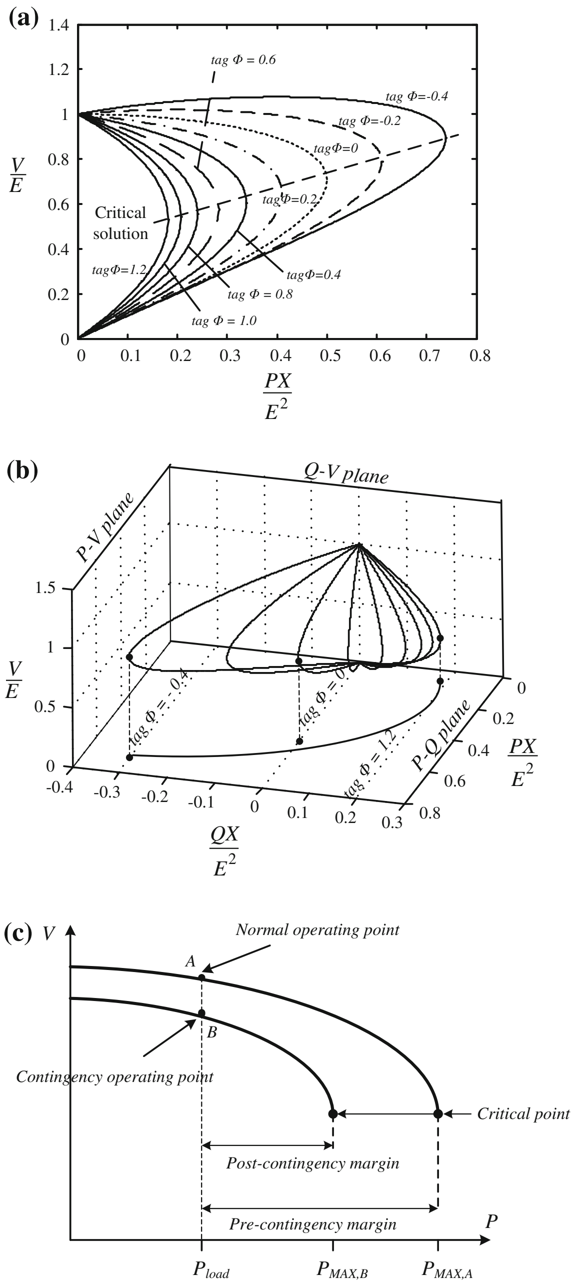

where all PV-curves displayed in Fig. 11.2a are plotted in a 3D graphic in order to identify the behavior of the reactive power Q, along with the behavior of active power P and voltage magnitude V.

Figure 11.2b includes 3 planes called *PV*, *QV* and *PQ*, respectively; the operative conditions are marked, considering the power factor and the critical voltage point:

1. Leading power factor, tan $\Phi = -0.4$. Under this condition, the load does not require reactive power from the system but it is producing it, this is denoted by the negative sign in *Q*, Fig. 11.2b.
2. Unity power factor, tan $\Phi = 0$. In this case the load is purely resistive. There are not reactive power consumption; the reactive power has a zero value.
3. Lagging power factor, tan $\Phi = 1.2$. Under this condition the load consumes both active and reactive power; this is the most common operating condition.

The projection of the operating points over the planes describes a specific curve, either *PV*, *QV* or *PQ*, for example the PV-plane shown in Fig. 11.2a.

The PV-curves method is also utilized in big power networks, but in that case the variable *P* represents the active power consumed by a full area in MW, and *V* becomes the voltage magnitude in pu Sometimes *P* can represent the active power of a transmission line. In this case, the *PV*-curve is calculated from a load flow calculation. For each specific condition a simulation is executed providing the voltage magnitudes. Several simulations are performed with different load conditions until a curve is built.

11.1.2 Voltage Stability Margin

The voltage magnitude is widely used as security criterion. Voltage levels are observed in simulations before and after an event occur. However, observing only the voltage levels may lead to an erroneous estimation. For this reason, besides of using such security criterion, it is necessary to define margins or distances that allow to predict in a precise way the real system condition, and to prevent the extent of possible changes in the system's operation, under common situations or disturbances [5, 6].

The concept of voltage stability margin has being introduced to reduce the risk of wrong estimations in the system condition. This concept may be defined as an estimation of the power system's proximity of experimenting problems due to bus voltage levels. In the last decade, important efforts have being performed to specify those margins in parameters of the power system that make practical sense to the grid operators.

In general, the voltage stability margin can be defined as the difference between a Key System Parameter (KSP) in the current operating point and the critical voltage stability point [7]. For instance, this KSP can be chosen as the active power, load reactive power, or the total flow capability of the system. There are several options to choose the KSP. However in practice there are two well established categories for this purpose:

1. Choosing the KSP based on the *PV*-curve, for example the total load in an specific area of the system, or the total power flow through a transmission line.
2. Choosing the KSP based on the *VQ*-curve, for example the reactive compensating power provided to a bus or group of buses.

The voltage stability margin is widely accepted to evaluate the voltage stability of a system; it has several advantages such as [8]:

- The concept of this index is not based on a particular model of the system, it can be used in either dynamic or static models independently of how detailed the model is.
- It is precise index which allows taking decisions regardless on the non-linearity of the system and the different device limits as the load is increasing.
- A sensitivity analysis can be applied to determine the effects over the parameters and control systems of the network [9].
- The margin considers the load increment model.

Another additional advantage of this margin is that voltage stability criteria can be defined, to determine how much margin is enough to ensure the system stability.

In general, this criterion may be defined as follows: "A power system can operate in such a way that for the current operating point, and with all possible contingencies, the voltage stability margin is larger than a certain percentage of the selected Key System Parameter" [7].

Figure 11.2c shows the calculation the voltage stability margin for different operating conditions, considering the KSP as the load modeled as constant power. The margin called *pre-contingency*, corresponds to a case where the power system is operated under normal conditions, which means the elements within the system are operating in a satisfactory way. The *post-contingency* margin is related to an undesired operation of the system, which means a perturbation has taken place in the system, for example a generator or a transmission line has tripped or other event that modifies the system operating conditions. Clearly, there is a wider margin in the pre-contingency case, and then there is confidence for operating the system under different circumstances.

Calculating the stability margin only for the pre-contingency case does not offer enough information from the security point of view, since this only describes the leading characteristics of the system for a particular case [10]. However, the analysis has to be complemented with the study of other cases, particularly the contingency cases, since for different reasons contingencies are inherent to the system operation.

From a strict point of view, it would be necessary to calculate the voltage stability margin for all possible contingencies that can take place inside the power system, taking into account either simple contingencies as well as complex events. But this takes a lot of time, and then the most important cases are typically analyzed.

For real-time or on-line analysis, the system state is known or approximately known through a variety of measurements and state estimation, and then the voltage stability margin is calculated considering a small list of contingencies. The selection of contingencies depends on the safety procedures used for each utility. The statistical data becomes a very useful.

In an off-line environment, where the time is not a constraint and long simulations can be carried out, it is necessary determining the voltage stability margin for a bigger number of contingencies, and also to consider some specific operative conditions, because frequently due maintenance trip of equipment the system rarely operates with all elements connected. For analysis purposes, each element out of service is combined with each contingency to get a set of double contingency simulations. With the result of those studies, sometimes databases are created for being utilized as a back-up for the system operators, with the objective to apply corrective actions for each contingency.

Some criteria established for different utilities are:

(a) Incremental/decremental criteria of voltage: specify that the voltage magnitude should stay within certain nominal range during all contingencies.
(b) Reactive reserve criteria: establish that the reserve of reactive power in a certain group of sources (generators, compensator devices, etc.) should be greater than a margin of their output power in all contingencies.

The combination of the aforementioned limits defines the operating limits; in other words, set the safety range that the system can be operated according to the voltage.

11.2 STATCOM at Steady State

The fundamental structure of the STATCOM is constituted by a Voltage Source Converter (VSC) and a coupling transformer which is utilized as link between the STATCOM and the power system, as illustrated in Fig. 11.3a.

The STATCOM may be considered the power-electronics version of a synchronous capacitor, it generates and injects reactive power into the system, but it can also absorb reactive power and it may change the amount of generated power in

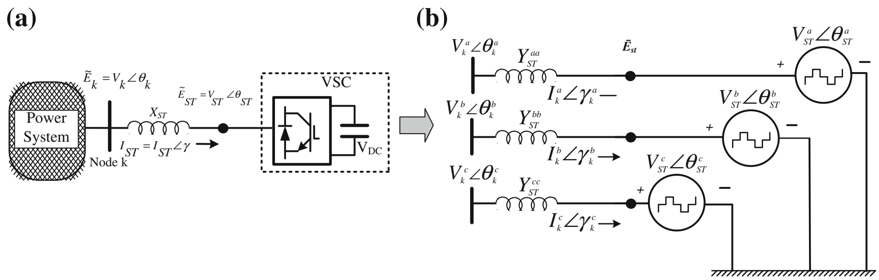

Fig. 11.3 **a** STATCOM basic structure. **b** Three-phase STATCOM equivalent circuit

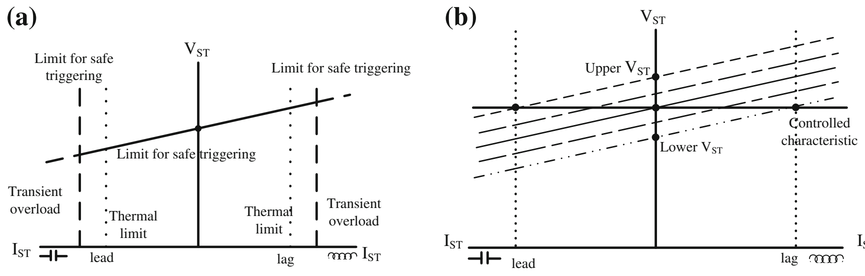

Fig. 11.4 **a** V-I STATCOM's profile. **b** V-I characteristic controlled by the STATCOM

a fast and continuous way; since it is not based on mechanisms, the principle of operation are very similar to a synchronous capacitor.

Figures 11.4a, b indicate that when the voltage generated by the STATCOM is lower than the voltage in the bus where this device is connected, the STATCOM behaves such an inductive load, absorbing reactive power from the grid. On the other hand, when the generated voltage is larger than the grid voltage, it behaves as a capacitive load, injecting reactive power into the system [11]. The STATCOM's losses are active power drawn from the grid; the amount of losses uses to be a small percentage of the device's rated power.

It would not be proper to connect the VSC terminals directly to the power system, which generally exhibits a larger short-circuit capacity. The STATCOM is coupled to the system through a set of inductors or a transformer to provide an inductive link to the grid; depending on the VSC, a set of harmonic filters can be included or a capacitors bank. In such cases also reactors may be used (separated from the coupling transformers), in order to limit the harmonic current from the converter to the capacitor bank.

The natural operation profile of voltage vs current in the STATCOM terminals is illustrated in Fig. 11.4a, this behavior depends fully on the voltage at the STATCOM terminals, and on the transformer or coupling reactance. The transformer reactance has typical values of 10–20 % of the STATCOM's capacity. In other words, the voltage drop is 10–20 % of the bus voltage when the STATCOM is operating at nominal current.

The current magnitude flowing through the Gate Turn-off Thyristors (GTO) or Insulated Gate Bipolar Transistors (IGBT) is independent of the phase this current has with respect to the bus voltage; those semiconductor devices also sustain any over-current only for a short time.

The maximum voltage that a STATCOM can hold at its terminals is usually 1.1 pu. However, the STATCOM can hold dynamic over-voltages and transients over the level provided by the over-voltage protective devices. During this transient condition, diodes in the VSC would allow the current to pass to the DC-link capacitor charging it to a higher value.

In practical applications, the STATCOM is expected to operate with a slope of about 2 and 5 %, Fig. 11.4a, which is smaller than the coupling transformer reactance, since the transformer reactance is constant, the voltage produced by the VSC in the STATCOM has to behave as shown in Fig. 11.4b.

When voltage V_{ST} increases until $V_{ST}(+)$ to attain a capacitive current, or reducing V_{ST} until $V_{ST}(-)$ to obtain a lagging condition (inductive current). This process can be rapidly achieved through properly handling the semiconductor devices, regulating the VSC's voltage magnitude if necessary [11].

The slope and the reactance, along with the output voltage in the VSC can be set to I_{ST} to control the scheme of the STATCOM, a set of characteristic slopes of voltage-current in the device for several voltage ranges. The STATCOM performance for voltage regulation is quite similar to the static VAr compensator (SVC), but in a more robust way, because the STATCOM operation is not related to low voltage conditions. Under reduced voltage levels the STATCOM can keep working in a leading or lagging way, in contrast to that, the current limits established for a conventional SVC are proportional to the voltage.

A STATCOM is a better option to provide reactive power to a power system, with low voltage problems, while the SVC can generally make more than the STATCOM to limit the dynamic over-voltages [11].

11.3 Embedding a STATCOM into the Power Flow Formulation

At steady state, the STATCOM can be represented in the same way as the synchronous capacitor, which most of the times is modeled as a synchronous generator in which the active power generated is zero. In the power flow problems, a more flexible model can be attained considering the STATCOM as a three-phase variable voltage source, in which the magnitude and phase angle can be regulated to get a constant voltage at the bus where the STATCOM is connected [12]. An expression for the voltage source of a three-phase STATCOM becomes

$$\mathbf{E}_{ST}^{\rho} = V_{ST}^{\rho}(\cos\theta_{ST}^{\rho} + j\ \mathrm{sen}\theta_{ST}^{\rho}) \tag{11.9}$$

where ρ indicates phase a, b, and c quantities; and "$_{ST}$" indicates STATCOM parameters. Figure 11.3b shows the three-phase STATCOM scheme, which can be interpreted as the three-phase Thevenin equivalent from the kth bus of the system.

Some steady state characteristics assumed for the STATCOM model are the following:

- The output voltage $\mathbf{E}_{ST}^{\rho}$ of the converter has only the fundamental frequency component, and then the STATCOM performance does not contribute with harmonic perturbations.
- The magnitude of the voltage V_{ST}^{ρ} is restricted by a maximum and minimum limit, which depends on the STATCOM capability. However, the phase angle θ_{ST}^{ρ} is not restricted to any value and can take values from 0 to 2π radians.

- Inside the power flow algorithms, the *k*th bus, where the STATCOM is connected, it is usually represented by a *PV* controlled voltage, which can change to a *PQ* load bus when the voltage magnitude exceeds the established limits.
- The effects of mutual inductances in the linking transformer between the STATCOM and the power system are neglected.

The circuit in Fig. 11.3b is used to derive the mathematical model of STATCOM, which will be used in the power flow formulation; based on that, the current in the circuit may be written as (11.10)

$$[\mathbf{I}_k^{\rho}] = \begin{bmatrix} \mathbf{Y}_{ST}^{\rho\rho} & -\mathbf{Y}_{ST}^{\rho\rho} \end{bmatrix} \begin{bmatrix} \mathbf{E}_k^{\rho} \\ \mathbf{E}_{ST}^{\rho} \end{bmatrix} \tag{11.10}$$

where:

$$\mathbf{I}_k^{\rho} = [I_k^a\angle\gamma_k^a \quad I_k^b\angle\gamma_k^b \quad I_k^c\angle\gamma_k^c]^t \tag{11.11}$$

$$\mathbf{E}_k^{\rho} = [V_k^a\angle\theta_k^a \quad V_k^b\angle\theta_k^b \quad V_k^c\angle\theta_k^c]^t \tag{11.12}$$

$$\mathbf{E}_{ST}^{\rho} = [V_{ST}^a\angle\theta_{ST}^a \quad V_{ST}^b\angle\theta_{ST}^b \quad V_{ST}^c\angle\theta_{ST}^c]^t \tag{11.13}$$

$$\mathbf{Y}_{ST}^{\rho\rho} = \begin{bmatrix} Y_{ST}^{aa} & 0 & 0 \\ 0 & Y_{ST}^{bb} & 0 \\ 0 & 0 & Y_{ST}^{cc} \end{bmatrix} \tag{11.14}$$

Based on (11.10) and (11.14), the next expression can be written for the active and reactive power injected into the *k*th bus:

$$P_k^{\rho} = (V_k^{\rho})^2 G_{ST}^{\rho\rho} + V_k^{\rho} V_{ST}^{\rho}\left[G_{ST}^{\rho\rho}\cos\left(\theta_k^{\rho} - \theta_{ST}^{\rho}\right) + B_{ST}^{\rho\rho}\mathrm{sen}\left(\theta_k^{\rho} - \theta_{ST}^{\rho}\right)\right] \tag{11.15}$$

$$Q_k^{\rho} = -(V_k^{\rho})^2 B_{ST}^{\rho\rho} + V_k^{\rho} V_{ST}^{\rho}\left[G_{ST}^{\rho\rho}\mathrm{sen}\left(\theta_k^{\rho} - \theta_{ST}^{\rho}\right) - B_{ST}^{\rho\rho}\cos\left(\theta_k^{\rho} - \theta_{ST}^{\rho}\right)\right] \tag{11.16}$$

The voltage source expressions become

$$P_{ST}^{\rho} = (V_{ST}^{\rho})^2 G_{ST}^{\rho\rho} + V_{ST}^{\rho} V_k^{\rho}\left[G_{ST}^{\rho\rho}\cos\left(\theta_{ST}^{\rho} - \theta_k^{\rho}\right) + B_{ST}^{\rho\rho}\mathrm{sen}\left(\theta_{ST}^{\rho} - \theta_k^{\rho}\right)\right] \tag{11.17}$$

$$Q_{ST}^{\rho} = -(V_{ST}^{\rho})^2 B_{ST}^{\rho\rho} + V_{ST}^{\rho} V_k^{\rho}\left[G_{ST}^{\rho\rho}\mathrm{sen}\left(\theta_{ST}^{\rho} - \theta_k^{\rho}\right) - B_{ST}^{\rho\rho}\cos\left(\theta_{ST}^{\rho} - \theta_k^{\rho}\right)\right] \tag{11.18}$$

Notice that for considering the STATCOM's variables in the load flow problem, two variables per phase are unknown, V_{ST}^{ρ} and θ_{ST}^{ρ}, and then six additional equations are required in the formulation.

The first equation is related to the active power restriction in the STATCOM, which may be absorbed, injected or being zero, which is included in (11.17). It is worth noting that the STATCOM cannot inject active power to the grid, unless it has a power generator or a long term energy storage element, usually a small amount of active power is drained into the STATCOM for compensating the losses in switching devices, capacitors, etc.

The second equation can be formulated considering the prevalent conditions in the power system bus where the STATCOM is connected. For instance, in Fig. 11.3b the STATCOM is connected to the kth bus for keeping constant the voltage magnitude V_k^ρ. Thus, V_k^ρ becomes a known parameter, in the power flow formulation it can be modeled as the voltage magnitude in the STATCOM terminals V_{ST}^ρ.

Linearizing (11.15) and (11.17) around the operating point becomes

$$\begin{bmatrix} \Delta P_k^\rho \\ \Delta Q_k^\rho \\ \Delta P_{ST}^\rho \end{bmatrix} = \begin{bmatrix} \frac{\partial P_k^\rho}{\partial \theta_k^\rho} & \frac{\partial P_k^\rho}{\partial V_{ST}^\rho} V_{ST}^\rho & \frac{\partial P_k^\rho}{\partial \theta_{ST}^\rho} \\ \frac{\partial Q_k^\rho}{\partial \theta_k^\rho} & \frac{\partial Q_k^\rho}{\partial V_{ST}^\rho} V_{ST}^\rho & \frac{\partial Q_k^\rho}{\partial \theta_{ST}^\rho} \\ \frac{\partial P_{ST}^\rho}{\partial \theta_k^\rho} & \frac{\partial P_{ST}^\rho}{\partial V_{ST}^\rho} V_{ST}^\rho & \frac{\partial P_{ST}^\rho}{\partial \theta_{ST}^\rho} \end{bmatrix} \begin{bmatrix} \Delta \theta_k^\rho \\ \frac{\Delta V_{ST}^\rho}{V_{ST}^\rho} \\ \Delta \theta_{ST}^\rho \end{bmatrix} \tag{11.19}$$

Then, the STATCOM is now integrated into the steady state model of the power system. From (11.19), the STATCOM account for a row and a column in the Jacobian matrix. The new elements of this matrix has the following expressions,

$$\frac{\partial P_k^\rho}{\partial \theta_k^\rho} = -Q_k^\rho - \left(V_k^\rho\right)^2 G_{ST}^\rho \tag{11.20}$$

$$\frac{\partial P_k^\rho}{\partial V_{ST}^\rho} V_{ST}^\rho = V_k^\rho V_{ST}^\rho \left[G_{ST}^\rho \cos\left(\theta_k^\rho - \theta_{ST}^\rho\right) + B_{ST}^\rho \mathrm{sen}\left(\theta_k^\rho - \theta_{ST}^\rho\right)\right] \tag{11.21}$$

$$\frac{\partial P_k^\rho}{\partial \theta_{ST}^\rho} = V_{ST}^\rho V_k^\rho \left[G_{ST}^\rho \cos\left(\theta_{ST}^\rho - \theta_k^\rho\right) + B_{ST}^\rho \mathrm{sen}\left(\theta_{ST}^\rho - \theta_k^\rho\right)\right] \tag{11.22}$$

$$\frac{\partial Q_k^\rho}{\partial \theta_k^\rho} = P_k^\rho - \left(V_k^\rho\right)^2 G_{ST}^\rho \tag{11.23}$$

$$\frac{\partial Q_k^\rho}{\partial V_{ST}^\rho} V_{ST}^\rho = V_k^\rho V_{ST}^\rho \left[G_{ST}^\rho \mathrm{sen}\left(\theta_k^\rho - \theta_{ST}^\rho\right) - B_{ST}^\rho \cos\left(\theta_k^\rho - \theta_{ST}^\rho\right)\right] \tag{11.24}$$

$$\frac{\partial Q_k^\rho}{\partial \theta_{ST}^\rho} = -V_k^\rho V_{ST}^\rho \left[G_{ST}^\rho \cos\left(\theta_k^\rho - \theta_{ST}^\rho\right) + B_{ST}^\rho \mathrm{sen}\left(\theta_k^\rho - \theta_{ST}^\rho\right)\right] \tag{11.25}$$

$$\frac{\partial P_{ST}^\rho}{\partial \theta_k^\rho} = \frac{\partial Q_k^\rho}{\partial V_{ST}^\rho} \partial V_{ST}^\rho \tag{11.26}$$

$$\frac{\partial P_{ST}^\rho}{\partial V_{ST}^\rho} V_{ST}^\rho = P_{ST}^\rho + \left(V_{ST}^\rho\right)^2 G_{ST}^\rho \tag{11.27}$$

$$\frac{\partial P_{ST}^\rho}{\partial \theta_{ST}^\rho} = -Q_{ST}^\rho - \left(V_{ST}^\rho\right)^2 B_{ST}^\rho \tag{11.28}$$

The STATCOM's reference voltage is set at the end of each iteration to ensure the voltage limits are not exceeded. If a limit is exceeded the magnitude voltage of the STATCOM terminal is set to the exceeded limit value, under this circumstances, in (11.19) V_{ST}^{ρ} is changed by V_k^{ρ}, which indicates that the voltage is no longer controlled in that bus. The linearized equation of the system is presented in (11.29)

$$\begin{bmatrix} \Delta P_k^{\rho} \\ \Delta Q_k^{\rho} \\ \Delta P_{ST}^{\rho} \end{bmatrix} = \begin{bmatrix} \frac{\partial P_k^{\rho}}{\partial \theta_k^{\rho}} & \frac{\partial P_k^{\rho}}{\partial V_k^{\rho}} V_k^{\rho} & \frac{\partial P_k^{\rho}}{\partial \theta_{ST}^{\rho}} \\ \frac{\partial Q_k^{\rho}}{\partial \theta_k^{\rho}} & \frac{\partial Q_k^{\rho}}{\partial V_k^{\rho}} V_k^{\rho} & \frac{\partial Q_k^{\rho}}{\partial \theta_{ST}^{\rho}} \\ \frac{\partial P_{ST}^{\rho}}{\partial \theta_k^{\rho}} & \frac{\partial P_{ST}^{\rho}}{\partial V_k^{\rho}} V_k^{\rho} & \frac{\partial P_{ST}^{\rho}}{\partial \theta_{ST}^{\rho}} \end{bmatrix} \begin{bmatrix} \Delta \theta_k^{\rho} \\ \frac{\Delta V_k^{\rho}}{V_k^{\rho}} \\ \Delta \theta_{ST}^{\rho} \end{bmatrix} \tag{11.29}$$

11.4 Case Study

Figure 11.5 depicts a schematic diagram of the New England system [13], which is being utilized as test system in this chapter.

New England scheme is referred to in the open research since represents an equivalent of 345 kV power system that interconnects New England area in the United States with the Canadian electrical system, which is composed by 10 equivalents generators, 39 buses and 46 transmission links (including transmission lines and transformers). This system has been widely studied from the voltage stability viewpoint [14, 15], the main reason for this is that presents an appropriate test system for different analysis. The shaded area is explained later in this chapter.

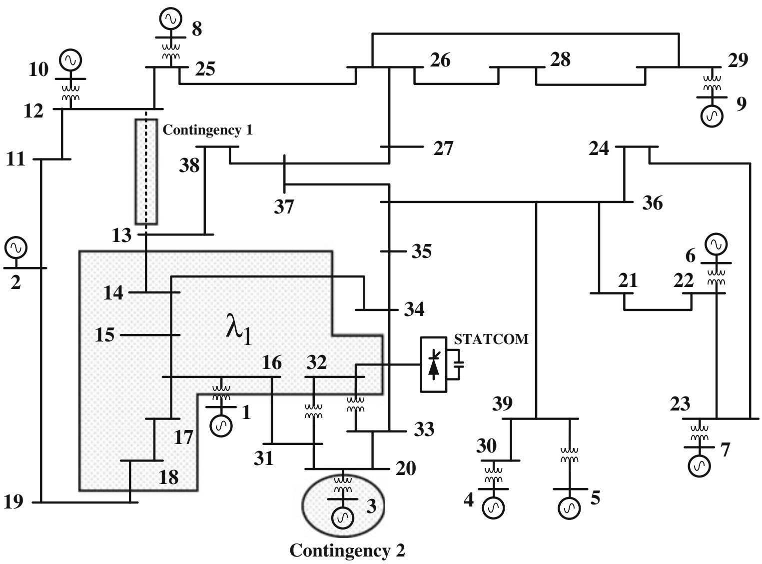

Fig. 11.5 One-line scheme of the test power system

The process to evaluate the voltage stability performance of the New England test system and the effects with the inclusion of the STATCOM mainly involves two steps:

1. Analysis of a reference case.
2. Analysis of three-phase unbalanced cases.

11.4.1 Analysis of the Reference Case

In order to establish a Base Case of Operation (BCOP) to study voltage stability, the analysis' aim of the BCOP is to determine the parameters that are used as a Ref. [16], and then quantify the variations of the reached results for other study cases. Then, it is important to take the following assumptions into account.

Each examined case is defined only on the basis of the interconnection scheme that prevails among the elements of the system. For the BCOP used in this chapter, the system operates with all its elements connected; this means that while the topology is not modified respect to the output of any element, such as a transmission line or a generator. The corresponding operating point is named BCOP. Contingencies are not assumed for the BCOP. Three-phase balanced parameters are another particular feature of the BCOP. Therefore, for such condition it is feasible to use a single-phase power flow analysis program. The main purpose of this assumption is to calculate some parameters as a reference for the unbalanced three-phase cases, without the need to take too much computational time.

A single-phase power flow program follows some recommendations [7], such as:

1. Capacities of Generators are represented by its reactive power limits.
2. Loads are established as constant power.
3. Taps of the transformers are kept in its nominal position.
4. Active power dispatch is fixed.
5. Single slack bus is utilized.

Regarding to the STATCOM characteristics, there are some premises included into the power flow algorithm:

- The bus where the STATCOM is connected is considered as conventional PV bus.
- The STATCOM's operating limits are function of voltage magnitudes kept in their terminals, and are: 1.1 pu as upper limit and 0.9 pu as lower limit. When the STATCOM violates any of these two limits, the voltage magnitude at its terminals is fixed at the violated limit value and the bus where it is connected, change from PV to PQ bus [17].
- The connection process between the STATCOM with the system is considered as instantaneous, this does not cause disturbances on other elements in the system,

and harmonic components that occur due to internal processes are neglected; just the fundamental frequency components are taken into account.

- The active power consumed by the STATCOM is zero, this is controlled by means of the phase angles corresponding to the terminals $\theta_{st} = \theta_k$. This is assumed in all simulations.

Proper management of single-phase power flow algorithm and taking advantage of factors that could be obtained, the next step in the analysis focuses to identify and define the weakest area in terms of voltage. In order to achieve this goal, nodal analysis can be executed [18]. If the most critical areas are properly identified along with their respective elements, then, the most severe operating conditions are identified, which may correspond to different topologies for these particular zones.

The methodology used to delimit the most vulnerable area in the New England test system is described in the following. Starting from an initial state of load, which for convenience is defined as "*current operating point*", an algorithm is implemented to overload the system until the "*critical point of voltage*" is reached. In other words, the algorithm reaches the condition when the system collapses. By modal analysis, the critical modes are a clear index to identify the loadability limit [8, 15, 17].

The procedure executed to bring the power system to an overload is that for building a PV-curve. This consists of increasing active and reactive power according to a specified weighting factor called "*K*". During the implemented simulation process, the load is gradually increased, according to the *K* factor. In each of these steps, power flow analysis is implemented and the attained solution is stored. For each operating point, the Jacobian matrix is calculated J_R [8, 18, 19], and its eigenvalue analysis is carried out. This is done with the aim of verifying the voltage stability condition. If the minimum eigenvalue calculated 'λ_{min}' is bigger than zero, the system is stable in terms of voltage, then power flow analysis is done again increasing the load. This procedure is repeated until the point of voltage collapse arises, which is achieved when 'λ_{min}' is equal to or less than zero.

Simultaneously with the power load increment, the active power generation is also augmented through the same "*K*" factor considered for the loads. Although this guess may not be regarded as realistic, numerical instability problems are avoided in the Newton–Rapshon algorithm [14]. As generators' active power increase, reactive power limits are changing as well; since it is considered that operate under a constant power factor.

Notice that some non-linearities are presented within the process. For instance, those related to the excitation system. Pragmatically, acceptable results have been shown using this technique, with a good approximation to the point of voltage collapse [8, 15, 17].

Once the critical point of voltage has been detected and with the power flow information, all necessary conditions for the voltage stability margin can be calculated; it is a function of the KSP. This margin is defined as the difference between the value of KSP at the current operating point and the critical point of collapse [7]. In the following analysis, the KSP is chosen as the total load active power of the system.

Thus, once the eigenvalues associated to the Jacobian matrix J_R, (λ_1, λ_2,…, λ_n), have been calculated, the purpose is to identify the critical modes [8, 18, 19]. In most cases, critical modes are selected based on the eigenvalues' magnitudes; while smaller the magnitude, lesser stable. It is noteworthy that the minimum eigenvalue calculated does not necessarily become the most critical mode, this is mainly due to some devices' non-linearities cannot be fully captured within the formulation. Although it is impractical and unnecessary to calculate all eigenvalues of the J_R matrix, it is recommended to verify 2–5 eigenvalues in detail [20], since if the smallest eigenvalues "*r*" are obtained along with their respective eigenvectors, then critical modes are obtained successfully. Regarding to this topic, significant progress has been presented in the applied mathematics, as well as in power systems in order to develop simulation algorithms that allow carrying out partial eigenvalues analysis [20–22].

Since New England test system used in the analysis is small compared to an actual power system with thousands of buses; modal analysis is made with conventional calculation routines, where only the critical mode is examined. For identifying critical modes, elements such as bus, transmission lines, and generator, with greater participation are classified. This is done calculating the factor defined as follows [16, 17]:

(a) Participation factor of a bus: $P_{ki} = \xi_{ki} n_{ik}$

(b) Participation factor of a branch: $PF^{(i)}_{branch\,km} = \dfrac{\Delta Q^{(i)}_{losses\,km}}{\max\left[\Delta Q^{(i)}_{system\,losses}\right]}$

(c) Participation factor of a generator: $PF^{(i)}_{GK} = \dfrac{\Delta Q^{(i)}_{GK}}{\max\left[\Delta Q^{(i)}_{G,\,system}\right]}$

where; 'ξ_{ki}' and 'η_{ik}' are the right and left eigenvectors, respectively.

Through the calculation of these factors, the location of weakest elements within the structure of the system is determined. Some study cases are selected as follows:

- Contingencies to study (output of a transmission line or generator)
- Selection of a bus where the STATCOM is connected.

Once the factors have been established, the most vulnerable area under voltage stability can be delimited and on which implementation of corrective actions must be focused.

Thus, for this analysis, the followed steps become:

1. Specify particular operating conditions.
2. Load increment until the critical point of collapse is detected.
3. Calculation of voltage stability margin.
4. Execute modal analysis.
5. Calculate participation factors.
6. Selection of contingencies, buses to compensate and the most vulnerable area.

These listed steps are applied only for the BCOP; thus modal analysis is mainly utilized to delimit the area of interest for voltage stability study. Then, for the cases

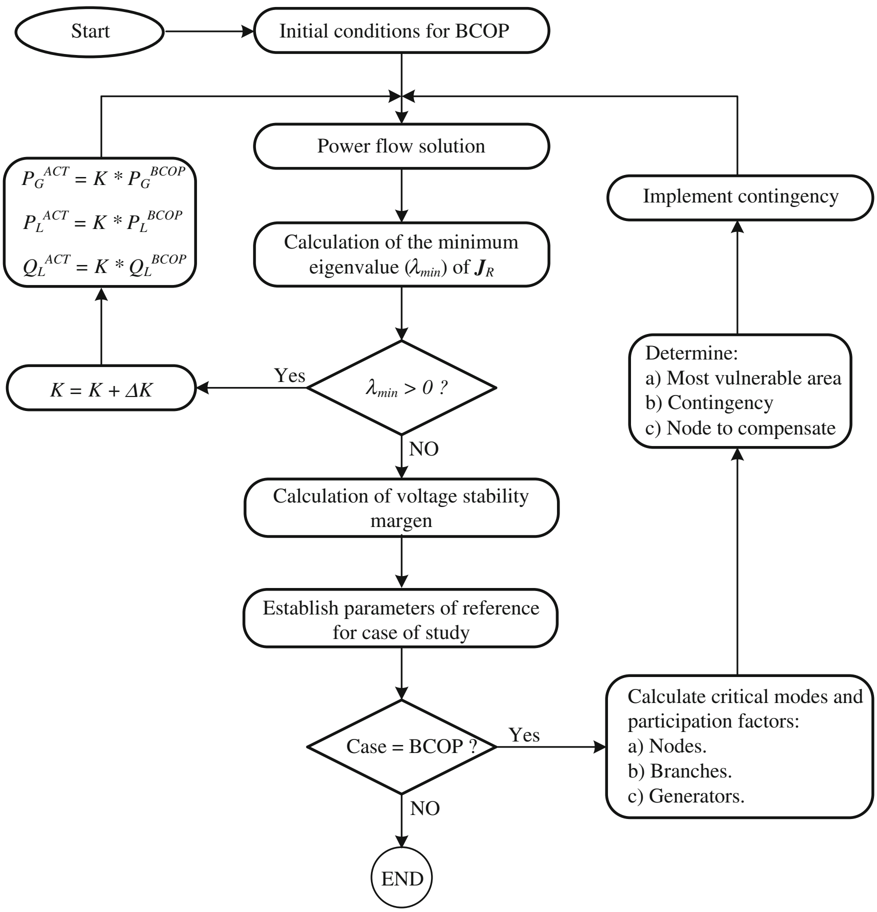

Fig. 11.6 Flowchart to establish reference parameters

where contingencies are deployed, steps 1–3 are applied. Figure 11.6 displays a flowchart of the above-mentioned procedure.

The superscript BCOP indicates original parameters of the current operating point. On the other hand, the superscript ACT, denotes updated values.

11.4.2 Analysis of Three-Phase Unbalanced Cases

Unbalanced operating conditions for steady state three-phase cases are discussed below. In general, the assumptions for single-phase power flow algorithm are also applied to the three-phase power flow study. The specific characteristics that need to be mentioned for this case are as following:

- In order to take into account STATCOM's limits into the three-phase formulation when it operates under unbalanced conditions, once any of its three-phases has violated voltage magnitude limits, automatically the three-phases are placed at the value of the violated limit. The STATCOM's controls do not consider independence between phases, in other words, it only has one degree of freedom. Same concept applies for the generators' reactive power limits.
- Loads are modeled as constant power and they are considered as star neutral connection to ground.

Figure 11.7 describes the essence of the implemented methodology to evaluate voltage stability limits over a three-phase reference frame. For example, factor K is applied in equal magnitude for all three-phases of each load. Therefore, before executing the routine, an unbalance of load is processed, Fig. 11.7.

Regarding to the eigenvalues calculation, 'n_l' describes the number of existing load buses. For the single-phase case, the Jacobian matrix J_R has dimension of ($n_l \times n_l$) with 'n_l' eigenvalues. Hence, on the three-phase case, J_R has dimension ($n_l \times 3 \times n_l \times 3$), with the corresponding '$n_l \times 3$' eigenvalues, where these values may be real or complex conjugates. For this application, just eigenvalues with real part are taken into account, discarding the complex conjugates.

According to the defined criteria to assess the system stability,

- If $\lambda_i > 0$, the system is stable in terms of voltage.
- If $\lambda_i < 0$, the system experiences a condition of voltage instability.
- If $\lambda_i = 0$, this is a voltage collapse condition.

The value and sequence that is attained for each eigenvalue (real or complex conjugates) cannot be determined with precision because it depends on the specific operating condition. In addition, based on the study of different cases, the number of eigenvalues with real part decreases while load is augmented considerably, which leads to an increment of the complex conjugate eigenvalues.

Acceptable results are obtained taking into account only eigenvalues with real part considering a three-phase analysis as shown bellow. This can be concluded based on comparison done with the single-phase analysis, where there is not the case of having complex conjugate eigenvalues, unless the system has a condition of voltage instability fully identified.

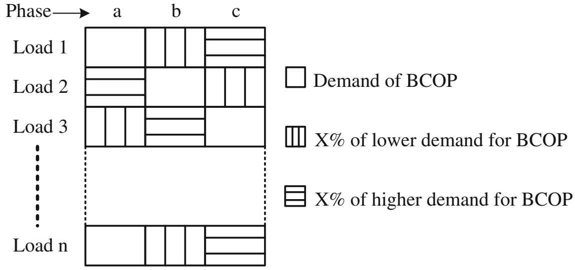

Fig. 11.7 Strategy to implement unbalanced conditions

The calculation of the participation factor is no longer performed for the three-phase analysis; however, a detailed analysis of system's parameters is done to implement the selected contingencies, considering compensation with the STATCOM as well without it. Outlines of the implemented steps are summarized in Fig. 11.8.

11.4.3 Results

In this section, simulating results are presented for the above-mentioned methodology applied to the New England power system, on which the performance of the model used for the three-phase STATCOM is evaluated and its impact on voltage stability. Initially, single-phase case is discussed to use it as a reference, then, an evaluation is reviewed for three-phase unbalanced cases. The synchronous machine 4th order model is used, equipped with an excitation system and a governor; its parameters are taken from [14]. Loads are modeled as constant power. Newton Raphson and Runge Kutta are used to solve the algebraic and differential equations, respectively.

11.4.3.1 Single-Phase Analysis

Some features assumed for the BCOP of New England system have already been defined. Some established conditions are taken into account for its analysis:

- The contingencies are not implemented; therefore, the system normally operates with all its elements.
- Balanced three-phase system.
- Original conditions of total load correspond to 6,126.5 MW and 1,593.4 MVAr. These load are taken as a reference to define the *current operating point* [2].
- Slack generator corresponds to the one installed on bus one illustrated in Fig. 11.5
- Unlike other researchers that have used New England as a test system for voltage stability study, here transformers of generators are not removed from the analysis, since they are a fundamental factor to balance total losses that prevail in the system. As above-mentioned, these transformers as well as those in the transmission network are considered with their taps at the nominal positions.

11.4.3.2 Voltage Stability Margin Calculation

In accordance to the flowchart depicted in Fig. 11.8, the analysis begins with the routine of overload until critical point of voltage collapse is detected for the BCOP. Within the algorithm, the factor K is specified with an increment of $K = 0.01$;

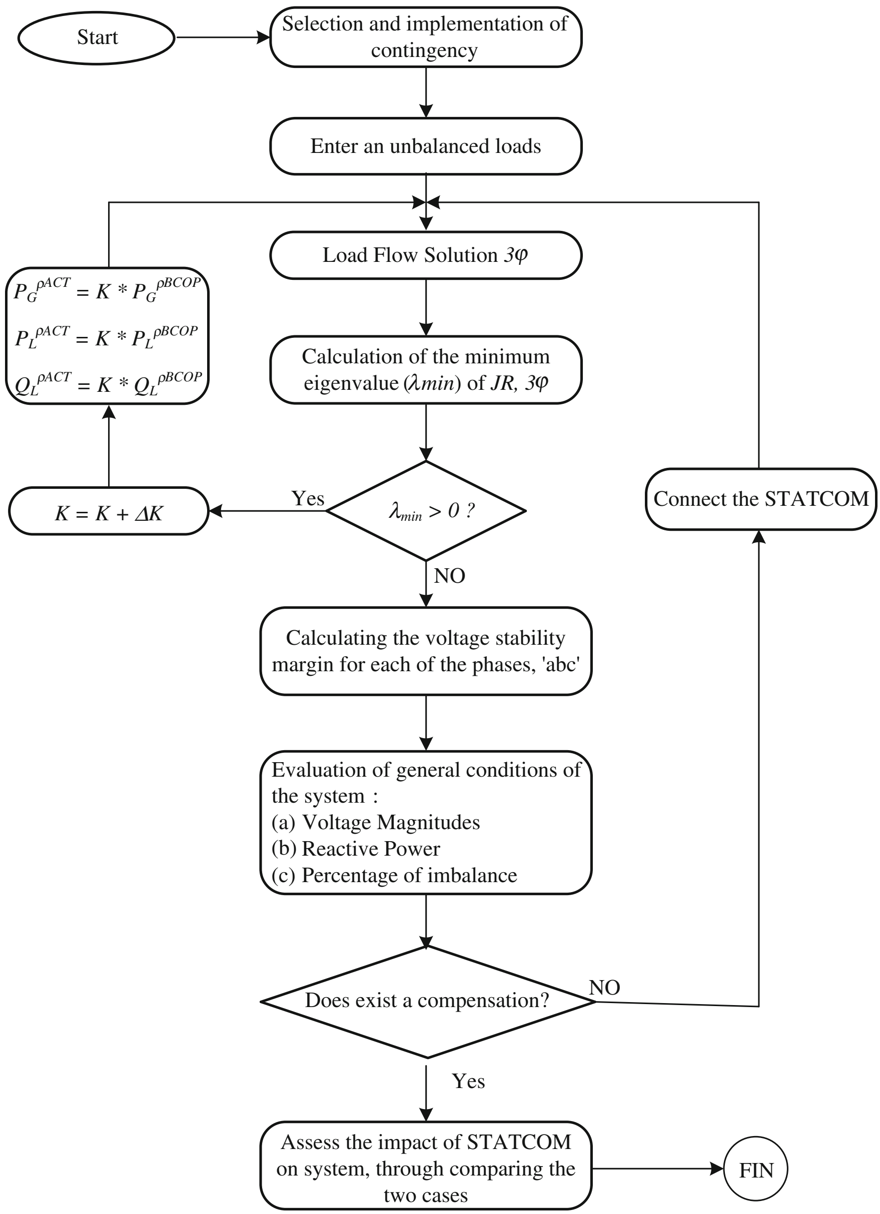

Fig. 11.8 Flowchart of the implemented steps for three-phase analysis

then, this factor remains constant throughout the routine. Therefore, each load is increased by 1 % on their original value. This procedure allows the calculation of the PV-curve for the BCOP. It is worth noting that this factor is the same for all cases simulated.

PV-curves generally depict the active power of total load in MW versus voltage magnitude on any bus of the system in per unit. Therefore, for this purpose it is necessary to choose a bus test.

Table 11.1 summarizes the solution for the BCOP through single-phase power flow algorithm. From this information, voltage magnitudes are analyzed for all load buses. Column four and five correspond to the active and reactive generated power, respectively. Column six and seven represent the active and reactive load power, while last column corresponds to the type of node (1–slack; 2–PV, 3–PQ). Notice that bus 32 has the smallest magnitude with value of 0.9397 pu Thus, this bus is chosen as test bus to plot PV-curves. This process is arbitrary and it is not an established rule; a similar result is obtained to choose another bus in the system without losing the generality of the PV-curve. On the other hand, the calculation of a complete PV-curve is usually not required in conventional studies for planning and operation [16]. According to this recommendation, only the top of the PV-curve is depicted, corresponding to all cases where the system is stable. Figure 11.9 illustrates the PV-curve getting for the BCOP.

Power flow results correspond to an operation condition with all elements of the system in operation, where:

- $|V|$, P_G, Q_G, P_D, Q_D, in (pu).
- θ in degrees.

Type1 = Slack; Type 2 = PV; Type 3 = Q.

The load condition for reaching the collapse, corresponds to 9,725.7 MW and 2,530.3 MVAr. These load values are taken as a reference to define the critical voltage point to the BCOP.

From Fig. 11.9 the voltage stability margin may be estimated; this value corresponds to 3,601.2 MW, which is equivalent to a load increment of 58.8 % over the BCOP.

The advantages of the PV-curve calculation for the BCOP's analysis are clear. There are two operating points that are of particular concern.

1. *Current operating point.*
2. *Critical voltage point.*

Subsequently more cases are defined, each one have their respective operating points to be analyzed (current and critical ones).

11.4.3.3 Modal Analysis

From the prevailing conditions for the BCOP's critical voltage point, modal analysis is performed. The following features are ascertained: if New England power system is considered without generators buses, the system comprises a total of 29 buses to be analyzed.

Tables 11.6, 11.7, 11.8 and 11.9 summarize information related to different parameters of modal analysis for BCOP. Note that provided data, have been

Table 11.1 Steady state solution

Bus	|V|	Θ	P_G	Q_G	P_D	Q_D	Tipo
1	1.0000	0	5.5167	2.0657	0.0920	0.0460	1
2	1.0300	−10.6993	10.000	2.1354	11.040	2.5000	2
3	0.9830	2.5108	6.5000	1.4449	0.0	0.0	2
4	1.0120	3.4129	5.0800	1.5308	0.0	0.0	2
5	0.9970	4.4336	6.3200	0.8011	0.0	0.0	2
6	1.0490	5.4360	6.5000	2.7532	0.0	0.0	2
7	1.0640	8.2210	5.6000	2.2921	0.0	0.0	2
8	1.0280	2.0914	5.4000	0.2430	0.0	0.0	2
9	1.0270	7.7804	8.3000	0.5811	0.0	0.0	2
10	1.0480	−3.7611	2.5000	1.8007	0.0	0.0	2
11	1.0355	−9.0557	0.0	0.0	0.0	0.0	3
12	1.0178	−6.1924	0.0	0.0	0.0	0.0	3
13	0.9879	−9.1862	0.0	0.0	3.2200	0.0240	3
14	0.9545	−10.1203	0.0	0.0	5.0000	1.8400	3
15	0.9572	−8.8885	0.0	0.0	0.0	0.0	3
16	0.9591	−8.1285	0.0	0.0	0.0	0.0	3
17	0.9507	−10.5488	0.0	0.0	2.3380	0.8400	3
18	0.9512	−11.1032	0.0	0.0	5.2200	1.7600	3
19	1.0097	−10.9152	0.0	0.0	0.0	0.0	3
20	0.9627	−5.3847	0.0	0.0	0.0	0.0	3
21	0.9859	−4.0964	0.0	0.0	2.7400	1.1500	3
22	1.0153	0.4294	0.0	0.0	0.0	0.0	3
23	1.0128	0.1566	0.0	0.0	2.7450	0.8466	3
24	0.9748	−6.5530	0.0	0.0	3.0860	0.9220	3
25	1.0266	−4.7182	0.0	0.0	2.2400	0.4720	3
26	1.0135	−5.9545	0.0	0.0	1.3900	0.1700	3
27	0.9932	−8.0732	0.0	0.0	2.8100	0.7550	3
28	1.0172	−2.2195	0.0	0.0	2.0600	0.2760	3
29	1.0195	0.7022	0.0	0.0	2.8350	0.2690	3
30	0.9843	−1.7746	0.0	0.0	6.2800	1.0300	3
31	0.9601	−6.3223	0.0	0.0	0.0	0.0	3
32	0.9397	−6.3025	0.0	0.0	0.0750	0.8800	3
33	0.9602	−6.1649	0.0	0.0	0.0	0.0	3
34	0.9586	−7.9833	0.0	0.0	0.0	0.0	3
35	0.9590	−8.2865	0.0	0.0	3.2000	1.5300	3
36	0.9751	−6.6434	0.0	0.0	3.2940	0.3230	3
37	0.9830	−7.8488	0.0	0.0	0.0	0.0	3
38	0.9834	−8.8315	0.0	0.0	1.5800	0.3000	3
39	0.9852	−0.7757	0.0	0.0	0.0	0.0	3

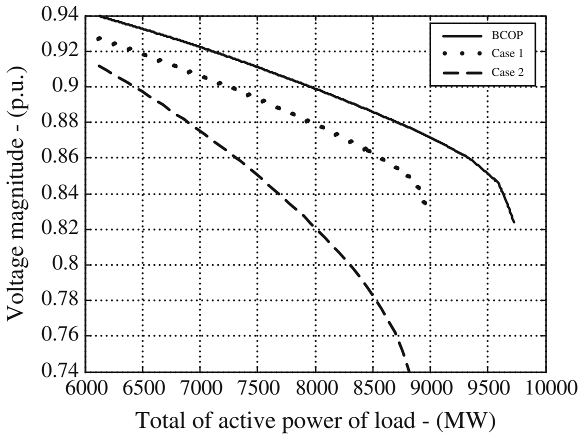

Fig. 11.9 PV-curves at bus 32

Table 11.2 BCOP's critical modes

Mode	Magnitude
1	5.9840
2	13.5383
3	26.1270
4	26.9969
5	39.2448

calculated on the basis of specific conditions for the BCOP's critical point, which corresponds to 9,725.7 MW and 2,530.3 MVAr. Table 11.2 illustrates the 5 modes less stable.

All these modes are positive, indicating that the system is stable in terms of voltage. However, if an extra iteration is made with their respective factor, some negative and complex conjugate eigenvalues will appear, denoting an instability voltage condition.

After that, the bus that are strongly related to the less stable modes are determined. This is done by calculating the participation factor 'FP_n', just for the two less stable modes. Table 11.3 depicts results of the participation factor of bus 'FP_n'.

The main result got from the analysis of participation factor of the bus, draws two areas exposed to problems of voltage stability. The area associated to mode 1 is considered more vulnerable. Buses associated with this area are remarked in Table 11.3, and the buses that are closer to generator 1, Fig. 11.5. In other words, those buses are the most significant modes that influence on the behavior of this phenomenon. Another advantage of this study is that allows determining the bus where the STATCOM should be connected. Since its magnitude is a measure of effectiveness that can be obtained by applying corrective measures. In this case, bus number 32 is selected for the STATCOM allocation.

Regarding to the contribution of transmission lines and generators on the problem, the participation factor of branches 'FP_{branch}' corresponding to mode 1

Table 11.3 Participation factors of buses for BCOP

Mode1		Mode 2	
Bus	FP_n	Bus	FP_n
32	0.1069	27	0.1046
17	0.0664	32	0.1031
34	0.0662	26	0.0727
14	0.0658	37	0.0713
18	0.0642	24	0.0635
15	0.0596	38	0.0539
33	0.0587	36	0.0529
31	0.0554	21	0.0522
16	0.0543	28	0.0475

Table 11.4 Participation factors of branches for mode 1 of BCOP

Transmission line		FP_{branch}
Sending bus	Receiving bus	
36	39	1
12	13	0.8545
18	19	0.8102
19	2	0.5506
21	22	0.4367
13	14	0.4043

Table 11.5 Participation factors of generators for mode 1 of BCOP

Bus	FP_{gen}
3	1
2	0.5777
6	0.5498
10	0.4365
5	0.4297
9	0.3539
8	0.3207
7	0.3199

are evaluated. Results are shown in Table 11.4, while the participation factors of generators 'FP_{gen}' are summarized in Table 11.5.

The participation factors of branches and generators help to determine contingencies that are implemented in simulations. This is a very important point in a voltage stability study, since contingencies are inherently related to the power system operation. In this context two contingencies are selected,

1. Transmission lines tripping.
2. Generators tripping.

In the case of a transmission line tripping, the used criterion is according to the line that exhibits greater participation for the mode under study. Regarding to data of Table 11.4, line 36–39 should be chosen using the mentioned criterion; however, generators 4 and 5 are excluded if this contingency is implemented; since this line links these generators, Fig. 11.5. Hence, this option is discarded. The following option corresponds to the transmission line linking buses 12–13. Although both transmission lines are identified, only one is implemented on the three-phase simulations. On the other hand, the chosen contingency for a generator's tripping becomes the number 3, since is the closest one to the study area. These two contingencies represent severe conditions for the mode under analysis.

In summary, applying modal analysis to the test system, the final result is represented graphically in Fig. 11.5, where it marks the weaker area through the shaded zone associated with the less stable mode. Additionally, two specific contingencies are stated, and the STATCOM's allocation for cases where compensation is required.

According to the algorithm established in Fig. 11.6, particular characteristics are defined for the analyzed cases:

- Case 1: BCOP.
- Case 2: A transmission line contingency.
- Case 3: A generator contingency.

For the three study cases, the current operating point, utilized to calculate PV-curves, the load level is 6,426.5 MW and 1,593.4 MVAr. Therefore, the difference among cases lies on the topology and not on the load level. In addition to the established objectives, the single-phase procedure determines the following parameters:

(a) Voltage stability margin.
(b) Level of voltage magnitude.
(c) Powers in the system.

Some BCOP parameters have already been calculated in the previous section and for the sake of brevity the details for cases 2 and 3 are omitted. Overall, the methodology used in these cases for calculating the PV-curves is done by running the routine when the system is overloaded. Figure 11.9 displays the PV-curves for the three cases. The bus under study is 32.

In Table 11.6, the results of the voltage stability margin for each case are summarized.

Table 11.6 Range of voltage stability (MW)

Case	Current operating point	Critical voltage point	Margin
1	6,126.5	9,725.7	3,601.2
2	6,126.5	8,960.1	2,835.6
3	6,126.5	8,819.3	2,696.8

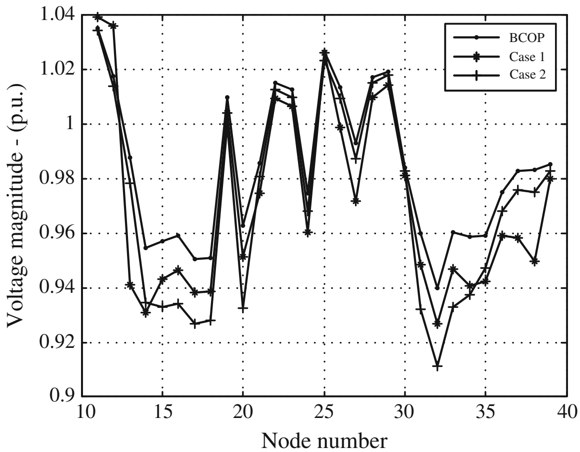

Fig. 11.10 Voltage magnitude at the load buses

Based on Table 11.6, for case 2 the voltage stability margin decreases by about 21 % compared to the BCOP, equivalent to a reduction of 765.6 MW. For case 3, the margin is reduced by 25 %, 906.4 MW lower than the BCOP. Regarding to the voltage magnitude, Fig. 11.10 exhibits the changes experienced by load bus when the system is subjected to operating conditions involving different study cases.

The "current operating point" is taken as a reference of the load conditions for calculating the parameters shown in Fig. 11.10. Generating voltages at buses (1–10) are not shown, since for these load conditions are constant. In Fig. 11.11a, the behaviour of powers is presented, while Fig. 11.11b presents the system losses.

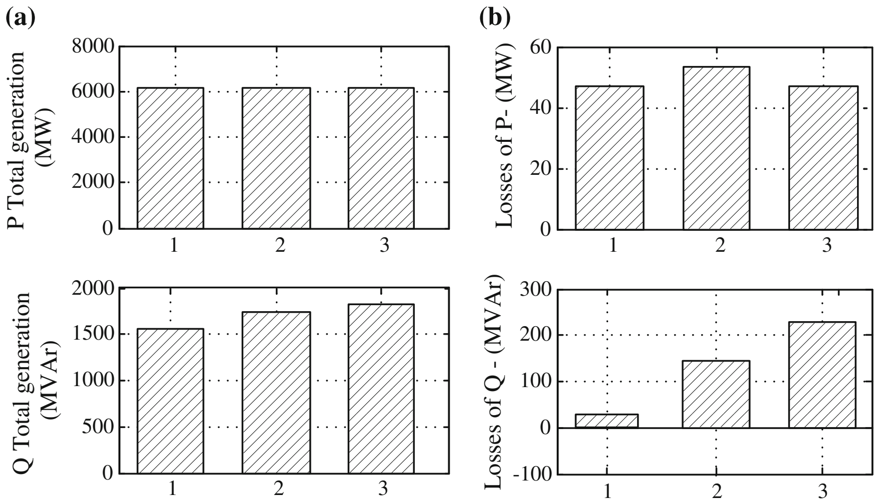

Fig. 11.11 **a** Total generation powers. **b** Total system losses

Furthermore, considering the load condition of the current operating point as a reference, it is possible to conclude that: The changes in the system topology result in minimal variations on the active power behaviour compared with those for the reactive power. It is for this reason that for the three-phase cases discussed in the next section, the analysis is focused only on reactive power changes.

Finally, single-phase simulations are also implemented considering the STATCOM within the system structure; these results are not shown graphically but are cited as references in the three-phase cases.

11.4.3.4 Unbalanced Three-Phase Cases

In this section, the three-phase STATCOM performance is evaluated; this is done through simulations involving severe operating conditions such as unbalanced overloads. One of the main objectives of this evaluation is to examine its operation effects on three-phase voltage stability margin and the voltage level prevailing at each bus, in addition to its overall impact on the system behaviour. According to the results obtained previously for the participation factors, one STATCOM is connected at bus 32. To identify each three-phase unbalanced study, the contingencies are subdivided as follows in the next four cases:

- Case 2a: Implementation of line contingency without compensation.
- Case 2b: Implementation of line contingency with compensation.
- Case 3a: Implementation of generator contingency without compensation.
- Case 3b: Implementation of generator contingency with compensation.

The compensated cases are referred to the STATCOM.

According to Fig. 11.7, the percentages of load unbalance become:

(a) Percentage of BCOP lower than the load: 1.7 %.
(b) Percentage of BCOP higher than the load: 3.2 %.

The New England test system has 19 load buses, which are illustrated in Table 11.1. Applying an unbalance factor to all loads through the specified sequence, Fig. 11.7, the total power demand is calculated, Table 11.7.

For the three-phase unbalanced cases, the power values shown in Table 11.7 are taken as the starting point of analysis. This is equivalent to the current operating point defined by the BCOP. Then cases 2a and 2b are compared. Following the flowchart shown in Fig. 11.8 for the four cases, the three-phase voltage stability margins are illustrated in Fig. 11.12.

Table 11.7 Total power of the unbalanced loads

Total active power (MW)			Total reactive power (MVAr)		
Phase *a*	Phase *b*	Phase *c*	Phase *a*	Phase *b*	Phase *c*
6,159.12	6,177.57	6,128.59	1,606.87	1,600.33	1,598.78

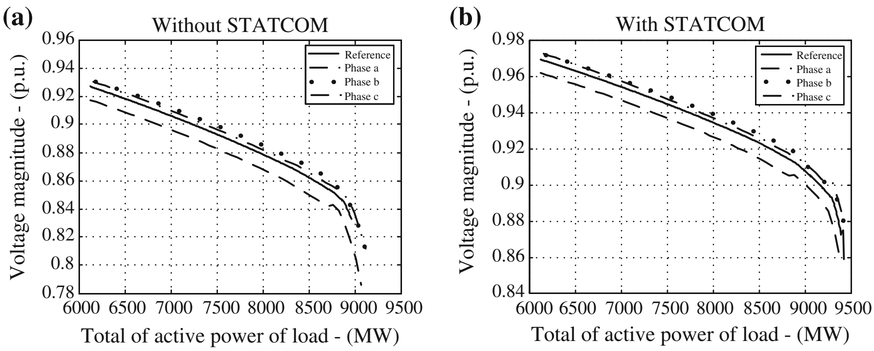

Fig. 11.12 Three-phase voltage stability margins at bus 32. **a** Case 2a; **b** Case 2b

Table 11.8 Voltage stability margins (MW)

Case	Single-phase	Three-phase		
		Phase *a*	Phase *b*	Phase *c*
2a	2,835.6	2,956.4	2,965.2	2,941.7
2b	3,295.1	3,266.4	3,276.1	3,248.2

According to these PV-curves, notice the difference between the attained results for calculating the voltage stability margin considering a single-phase respect to three-phase unbalanced condition. In both cases, the references correspond to that for the single-phase operating condition. Table 11.8 shows the results for different margins, according to the case and the considered phase.

Analysing Table 11.8, notice that depending on the operating conditions and the reference frame in question, different effects arise. For example, for Case 2a, the single-phase reference corresponds to 2,835.6 MW, and instead the three-phase results reveal that the margin is around 2,950 MW per phase; there is a difference of 100 MW between both cases. Furthermore, for Case 2b, the calculated three-phase condition, the margin is lower than that of the single-phase case in an average of 40 MW per phase. This means that in order to get results closer to the actual system, it is necessary to take into account these unbalances.

Note in Fig. 11.12, phases *a* and *b*, that there is a significant unbalance between the voltage magnitudes, regardless the STATCOM operation [16]. It is assumed that the STATCOM is able to keep the voltage magnitude at bus 32 in 1 pu; this is a significant constraint for the demanding conditions of the original test system. The remaining STATCOM's parameters used in these simulations are shown in Table 11.9.

Table 11.9 STATCOM data

Bus	R_{stat}	X_{stat}	V_{esp}	V_{max}	V_{min}
32	0.0	0.1	1.0	1.1	0.9

where:

R_{stat} is the coupling transformer's resistance (pu).
X_{stat} is the coupling transformer's reactance (pu).
V_{esp} desired voltage magnitude at bus 32 (pu).
$V_{\max}$ STATCOM terminal voltage upper limit (pu).
$V_{\min}$ STATCOM terminal voltage lower limit (pu).

Separating each of the stages shown in Fig. 11.12a, b, corresponding to bus 32, the results in Fig. 11.13 are obtained.

Figures 11.13a–c clearly indicate the STATCOM's effects at the compensated bus. Figures show that although operating limits are violated, the STATCOM increases the voltage stability margin by an average of 10 % per phase, which for the analysed cases, corresponds to 300 MW. Furthermore, the voltage magnitude is improved about 5 %, equivalent to 0.05 pu, and this factor is maintained throughout the overload process, which verifies that the STATCOM operation is unaffected by the low-voltage at the bus where it is connected.

STATCOM impacts on the general system's conditions. An overview of voltage levels at the load buses per-phase is illustrated in Fig. 11.14. The operating conditions taken into account for calculating these signals are presented in Table 11.7.

The voltage magnitudes in Fig. 11.14 imply that the effects of STATCOM are higher at the bus where it is connected; such effects are less on the neighbor buses.

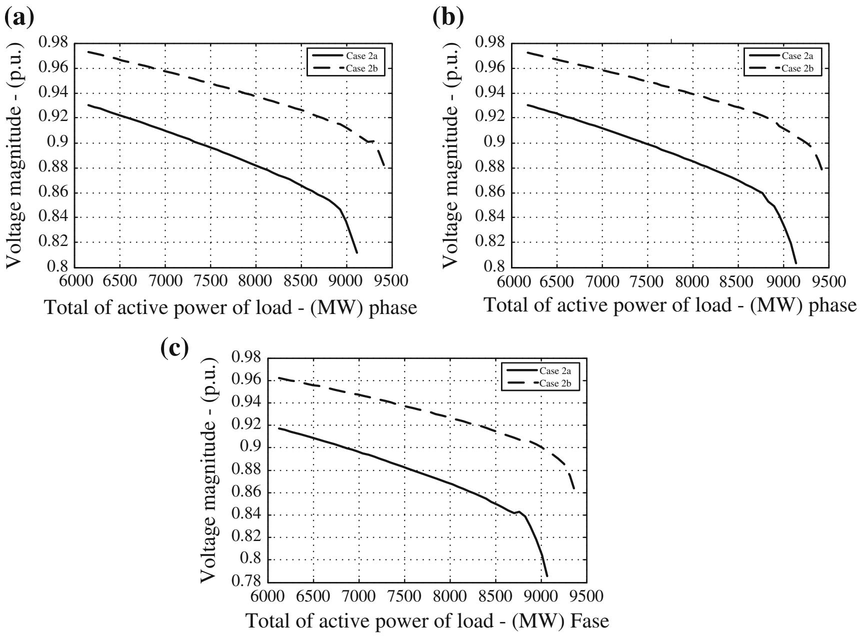

Fig. 11.13 Margins per phase at bus 32. Total of active power of load—(MW) phase (**a**). Total of active power of load—(MW) phase (**b**). Total of active power of load—(MW) Fase (**c**)

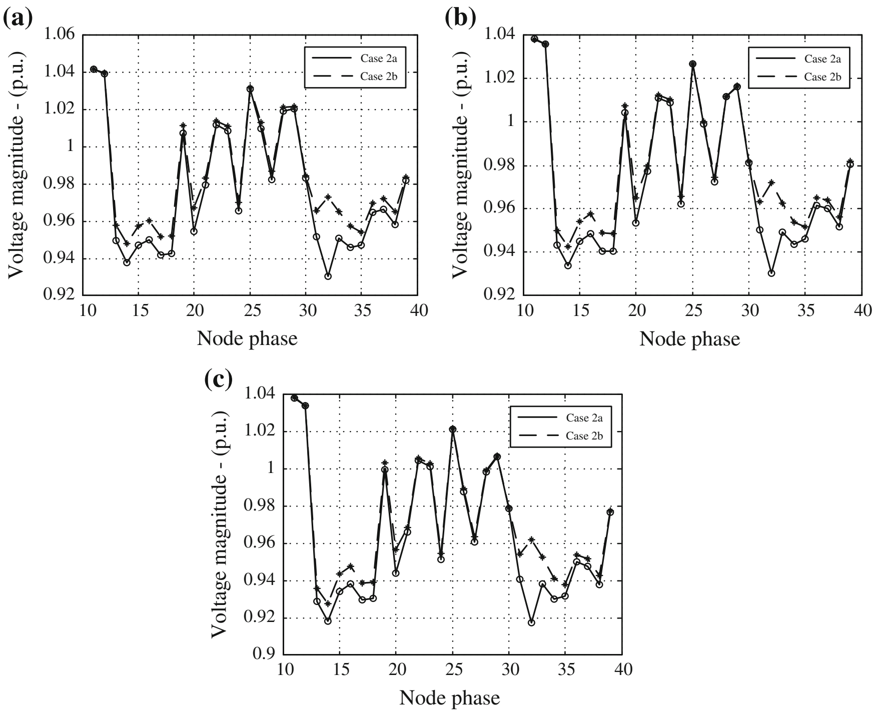

Fig. 11.14 Per phase voltage magnitude at load buses. Node phase (**a**). Node phase (**b**). Node phase (**c**)

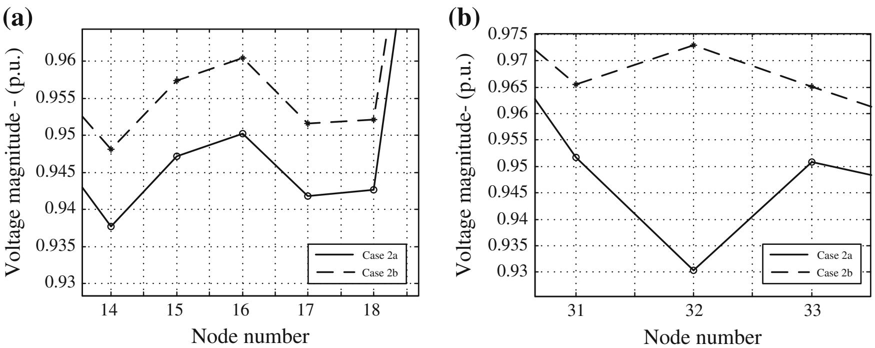

Fig. 11.15 Voltage magnitude at the buses of the weakest area, phase *a*

This can be noticed by referring to the bus involved in the shaded area in Fig. 11.5, identified as the most vulnerable area of the test system. Buses with a lower voltage level are 14–16 and 31–33, Fig. 11.14. A zoom of Fig. 11.14 is depicted in Fig. 11.15.

Table 11.10 Reactive power supplied by the generators (MVAr)

Case	Generator 1			Generator 3		
	Phase *a*	Phase *b*	Phase *c*	Phase *a*	Phase *b*	Phase *c*
2a	276.63	236.66	286.655	197.42	201.64	213.09
2b	237.52	195.46	250.76	136.77	141.55	150.89

Table 11.11 Reactive power supplied by the STATCOM, (MVAr)

Phase *a*	Phase *b*	Phase *c*
139.98	142.81	149.31

Notice from Figs. 11.14 and 11.15 that the results of the modal analysis are verified, because according to these principles, the specific location for the STATCOM, based on the most unstable mode should help to improve the operating conditions in those buses significantly associated with the critical mode. Similar behaviour can be observed for phases *b* and *c*.

A constant power load is assumed to analyse the reactive power behaviour in the system. The studied generators are those at buses 1 and 3. Table 11.10 presents the values of the generated reactive power for Cases 2a and 2b.

Fron Table 11.10 it follows that the STATCOM helps to reduce the reactive power output of generators. For example, the decrement in the generator 1 is about 15 %, and with respect to the generator 3, the reduction is approximately 30 %. With this, the possibilities that generators can achieve their operational limits, especially those for the excitation system are considerably reduced. These two generators are the most favoured by the inclusion of the STATCOM. In general, all generators diminish its reactive power output. The reactive power provided by STATCOM in case 2b is shown in Table 11.11. Likewise, the power losses in the transformers connected to bus 32 are summarized in Table 11.12.

In both transformers, the losses are significantly reduced, about 90 % for the transformer between buses 31–32, and about 80 % for the other, buses 32–33.

Table 11.13 illustrates total losses for cases 2a and 2b. In Tables 11.13 and 11.14 the following concepts stand for:

Margin: Stability voltage margin, (MW).
Magnitude: Voltage magnitude at bus 32, (pu).
Losses: Total reactive power losses, (MVAr).
V-STATCOM: Terminal voltage magnitude of the STATCOM, (pu).
Q-STATCOM: Active power generated by the STATCOM, (MVAr).

Table 11.12 Transformers' reactive power losses (MVAr)

Case	Transformers between buses 31–32			Transformers between buses 32–33		
	Phase *a*	Phase *b*	Phase *c*	Phase *a*	Phase *b*	Phase *c*
2a	1.0608	0.9455	1.2190	0.9312	0.8619	1.0028
2b	0.1371	0.1879	0.1704	0.1738	0.2031	0.2108

Table 11.13 Parameters corresponding to the line's contingency

Parameters	Without STATCOM			With STATCOM		
	Phase *a*	Phase *b*	Phase *c*	Phase *a*	Phase *b*	Phase *c*
Margin	2,956.4	2,965.2	2,941.7	3,266.4	3,276.1	3,248.2
Magnitude	0.9304	0.9325	0.9406	0.9729	0.9721	0.9621
Losses	111.98	138.29	216.68	78.38	113.98	185.83
V-STATCOM	–	–	–	1.1	1.1	1.1
Q-STATCOM	–	–	–	139.99	142.81	149.31

Table 11.14 Parameters corresponding to generator's contingency

Parameters	Without STATCOM			With STATCOM		
	Phase *a*	Phase *b*	Phase *c*	Phase *a*	Phase *b*	Phase *c*
Margin	2,956.4	2,965.2	2,941.7	3,266.4	3,276.1	3,248.2
Magnitude	0.9304	0.9325	0.9406	0.9729	0.9721	0.9621
Losses	111.98	138.29	216.68	78.38	113.98	185.83
V-STATCOM	–	–	–	1.1	1.1	1.1
Q-STATCOM	–	–	–	139.99	142.81	149.31

Notice that there is a notorious unbalance between phases, especially between *a* and *c*, which is about 100 MW. The total losses for Case 2a corresponds to 467.95 MVAr, while for Case 2b becomes 378.21 MVAr. Thus, the STATCOM contributes to improve the general system conditions. A similar analysis is performed for Cases 3a and 3b are summarized in Table 11.14.

References

1. Taylor CW (1996) Power system voltage stability. McGraw-Hill, New York
2. Padiyar KR (1995) Power system dynamics: stability and control. Wiley, New York
3. Van Cutsem T, Vournas C (1998) Voltage stability of electric power system. Kluwer, Norwell
4. Chua LO, Desoer CA, Kuh ES (1987) Linear and nonlinear circuits. McGraw Hill, New York
5. Gao B (1996) Towards the development of a systematic approach for voltage stability assessment of large-scale power systems. IEEE Trans Power Syst 11(3):1314–1324
6. Van Cutsem T et al (1999) Determination of secure operating limits with respect to voltage collapse. IEEE Trans Power Syst 14(1):327–333
7. IEEE/PES Power System Stability Subcommittee Special Publication (2002) Voltage stability assessment: concepts, practice and tools. IEEE/PES Final Document. ISBN 0780378695
8. IEEE/PES Power Systems Stability Subcommittee Special Publications (2001) Voltage stability assessment, procedures and guides, final draft. http://www.power.uwaterloo.ca. Accessed Dec 2013
9. Greene S et al (1999) Contingency ranking for voltage collapse via sensitivities from a single nose curve. IEEE Trans Power Syst 14(1):232–238

10. Repo S (2001) On-line voltage stability assessment of power system-an approach of black-box modelling. Ph.D. dissertation, Tampere University of Technology, Tampere
11. Song YH, Johns AT (1999) Flexible ac transmission system (FACTS). The Institution of Electrical Engineers, UK
12. Acha E, Fuerte-Esquivel CR, Ambriz-Pérez H, Ángeles Camacho C (2006) FACTS: modelling and simulation in power network. Wiley, England
13. Zhang XP, Xue CF, Godfrey KR (2004) Modelling of the static synchronous series compensator (SSSC) in three-phase power flow. IEE Proc Gener Transm Distrib 151 (4):486–494
14. Ajjarapu V, Christy C (1992) The continuation power flow: a tool for steady state voltage stability analysis. IEEE Trans Power Syst 7(1):416–423
15. Mansour Y, Kundur P (1991) Voltage collapse: industry practices: control and dynamic systems. Academic Press, Waltham
16. Gao B, Morison GR, Kundur P (1996) Towards the development of a systematic approach for voltage stability assessment of large-scale power systems. IEEE Trans Power Syst 11 (3):1314–1324
17. Ramirez Juan M, Murillo-Perez José L (2006) Steady state voltage stability with STATCOM. IEEE Trans Power Syst 21(3):1453–1454
18. Mansour Y (1993) Suggested techniques for voltage stability analysis. 93TH0620-5PWR, IEEE/PES
19. Ramírez Juan M, Murillo Jose L (2006) Three-phase voltage stability studies embedding a STATCOM. In: proceedings of the IEEE power engineering society general meeting, Montréal
20. Stewart William J, Jennings Allan (1981) A simultaneous iteration algorithm for real matrices. ACM Trans Math Softw 7(2):184–198
21. Wang L, Semlyen A (1992) Application of sparse eigenvalue techniques to the small signal stability analysis of large power system. IEEE Trans Power Syst 5(2):635–642
22. Martin N (1986) Efficient eigenvalue and frequency response methods applied to power system small-signal stability studies. IEEE Trans Power Syst 1(2):217–225